on results for corresponding cyclopropanes. Thus difluoro substitution, which lengthens the opposite bond in cyclopropane, does indeed favor the annulenic form of 1,6-methano[10]annulene, whereas dicyano substitution, which shortens the opposite bond in cyclopropane, does indeed favor the norcaradienic structure. For dichloro substitution, both theory and experiment predict a lengthening of the opposite bond in cyclopropane, similar to that observed for the difluoro derivative. On the other hand, dichloro substitution in the 1,6-methano[10]annulene system is found both theoretically and experimentally to favor, relative to the difluoro systems, the norcaradienic structure. The most plausible explanation for the different behavior of the fluoro and chloro substituents in the 1,6-methano[10]annulene system comes from noting that chlorine is considerably bulkier than fluorine and comparable in size to methyl: van der Waals' radii are[36] respectively 1.73, 1.47, and 1.80 Å. Thus steric interaction between the chloro substituents and carbon atoms 3, 4, 8, and 9 would contribute, just as in the case of methyl, to a preference for the norcaradienic structure, as observed. The theoretical calculations, in the absence of geometry reoptimization, would be expected to overemphasize such steric interaction in the annulenic form and this is also consistent with the results.

Concluding Remarks

Two minima have been located in the potential-energy surface of 1,6-methano[10]annulene that correspond to annulenic (**8**) and norcaradienic (**9**) structures. However, the barrier separating these forms is very small so that only the more stable annulenic valence isomer (**8**) is expected to be observable. The calculated structure for **8** agrees well with that obtained experimentally. The effect of substituents on the annulene (**8**)–norcaradiene (**9**) equilibrium is generally well described by the calculations. Hyperconjugative and hybridization effects similar to those operative in substituted cyclopropanes may be used to rationalize the observed preferences for norcaradienic and annulenic structures for cyano and fluoro substituents, respectively. For methyl and chloro substituents, steric effects are found to be important. In particular, for the dichloro derivative, this leads to a relative favoring of the norcaradienic structure, not expected on the basis of results for the model cyclopropane system.

Note Added in Proof. Since this paper was submitted, we have become aware of recently completed calculations, carried out at higher levels of theory, on the 1,6-methano[10]annulene system.[37] These higher level calculations show that (i) geometry optimization at the STO-3G (as opposed to STO-2G used here) level has a very small effect on the relative energies of **8** and **9**: values of 98 (Table I) and 97 (ref 37) kJ mol^{-1} are obtained at the STO-3G//STO-2G and STO-3G//STO-3G levels, respectively; (ii) geometry optimization at the 6-31G level also has a relatively small effect (thus the relative energies of **8** and **9** are 26 (Table I) and 23 (ref 37) kJ mol^{-1} at the 4-31G//STO-2G and 6-31G//6-31G levels, respectively); (iii) finally, incorporation of electron correlation leads, as expected, to a relative stabilization of the annulenic isomer **8**. The relative energy of **9** at MP2/6-31G//6-31G is 65 kJ mol^{-1}. This value is likely to be reduced at higher correlation levels (since MP2 generally overestimates correlation effects) and through addition of polarization functions to the basis set. Consequently, the energy difference between **8** and **9** is likely to lie between our 4-31G//STO-2G estimate of 26 kJ mol^{-1} and the MP2/6-31G value of 65 kJ mol^{-1}.

Registry No. **7**, 2443-46-1; 11-fluoro-1,6-methano[10]annulene, 71671-89-1; 11,11-difluoro-1,6-methano[10]annulene, 19026-91-6; 11-cyano-1,6-methano[10]annulene, 10474-26-7; 11,11-dichloro-1,6-methano[10]annulene, 19026-92-7; 11,11-dicyano-6-methano[10]-annulene, 61997-35-1; 11,11-dimethyl-1-methano[10]annulene, 58863-22-2.

(36) Bott, G.; Field, L. D.; Sternhell, S. *J. Am. Chem. Soc.* **1980**, *102*, 5618.

(37) Raghavachari, K.; Haddon, R. C.; Pople, J. A., paper presented at the 183rd American Chemical Society National Meeting, Las Vegas, NV, March 1982.

Analysis of the Kinetics of Electron Transfer between Blue Copper Proteins and Inorganic Redox Agents. Reactions Involving Bis(dipicolinate) Complexes of Cobalt(III) and Iron(II) and Stellacyanin, Plastocyanin, and Azurin

A. Grant Mauk,[1a] Emilio Bordignon,[1b] and Harry B. Gray*

Contribution No. 6550 from the Arthur Amos Noyes Laboratory, California Institute of Technology, Pasadena, California 91125. *Received October 26, 1981*

Abstract: The kinetics of electron-transfer reactions involving bis(dipicolinato)cobaltate(III) ($Co(dipic)_2^-$) and bis(dipicolinato)ferrate(II) ($Fe(dipic)_2^{2-}$) with Japanese *Rhus vernicifera* stellacyanin, *Phaseolus vulgaris* plastocyanin, and *Pseudomonas aeruginosa* azurin have been studied. Second-order rate constants (M^{-1} s^{-1}; 25 °C; pH 7.0 (phosphate), μ = 0.2 M), ΔH^* (kcal/mol), and ΔS^* (eu) values are as follows: 6.8 (2) × 10^4, 6.7 (5), and −14 (2) for stellacyanin(II)–$Fe(dipic)_2^{2-}$; 2.04 (8) × 10^4, 4.8 (4), and −23 (1) for plastocyanin(II)–$Fe(dipic)_2^{2-}$; 4.57 (7) × 10^2, 4.5 (2), and −31.2 (8) for plastocyanin(I)–$Co(dipic)_2^-$; and 9.8 (2) × 10^2, 4.5 (4), and −30 (1) for azurin(II)–$Fe(dipic)_2^{2-}$. The oxidation of stellacyanin(I) by $Co(dipic)_2^-$ was found to be too fast to measure, and rate saturation was observed for the azurin(I)–$Co(dipic)_2^-$ reaction. Protein reactivity parameters extracted from an analysis of the kinetics data for the oxidations of plastocyanin(I) and azurin(I) by $Co(dipic)_2^-$ and $Co(phen)_3^{3+}$ are interpreted in terms of a bimolecular electron-transfer mechanistic model in which protein–reagent binding is a dead-end (K = 46 (5) M^{-1} for azurin(I)–$Co(dipic)_2^-$). Estimated protein electron-transfer distances are about the same (~2–3 Å) for these reactions, suggesting that the hydrophobic π-conducting ligands penetrate the hydrophobic region around the copper–histidine redox units (His-87 in plastocyanin; His-117 in azurin); the distances based on reactions with hydrophilic reagents, however, are 2–3 Å larger for azurin than for plastocyanin, which is consistent with available structural data and the assumption that these redox agents cannot penetrate the three residues (Met-13, Met-44, Phe-114) that isolate copper (His-117) in azurin.

Previous studies in our laboratory have shown that the blue copper centers in the proteins Japanese *Rhus vernicifera* stellacyanin, *Phaseolus vulgaris* (bean) plastocyanin, and *Pseudomonas aeruginosa* azurin differ markedly in their reactivity with various

0002-7863/82/1504-7654$01.25/0

inorganic redox reagents.[2] Analysis of the kinetics of these reactions suggests that the copper site in stellacyanin is located at or very near the surface of the protein, whereas the sites in plastocyanin and azurin are less accessible to redox agents. The wide variations in reactivity among the three copper centers, whose electronic structures are very similar,[3] have been used to estimate the distances over which electron transfer takes place in the assumed reagent–protein outer-sphere activated complexes.[4] Within the framework of a bimolecular mechanistic model, anomalously high redox reactivity in plastocyanin or azurin is interpreted in terms of reagent penetration into the protein interior, thereby reducing the distance over which electron transfer occurs.

The mechanistic situation is more complicated for the oxidations of plastocyanin(I) and azurin(I) by $Co(phen)_3^{3+}$, as slight deviations from linearity in the plots of k_{obsd} vs. [oxidant] have been observed.[5] Such apparent rate saturation raises the possibility that electron transfer may occur by an intramolecular pathway within a precursor complex, and in that context there have been specific assignments of the productive binding sites on the plastocyanin and azurin surfaces. In the oxidation of plastocyanin(I) by $Co(phen)_3^{3+}$, for example, it has been suggested that copper(I) transfers an electron to an oxidant cation that is bound electrostatically at a site comprised of several carboxylate residues (the "negative patch") near Tyr-83.[6]

Because there are other plausible mechanistic interpretations of saturation kinetics,[7] we felt that the question of plastocyanin and azurin electron-transfer reactivity required further examination. As part of this examination, we have extended our previous studies of the kinetics of redox reactions of the three copper proteins to include $Fe(dipic)_2^{2-}$ and $Co(dipic)_2^-$ (dipic = dipicolinate); this reductant–oxidant pair was used successfully in probing the electron-transfer reactivity of *c*-type cytochromes,[8] and it should be helpful in sorting out certain of the mechanistic problems that remain unsolved in the case of blue copper proteins. In particular, the electron-transfer reactivity of plastocyanin(I) and azurin(I) with $Co(dipic)_2^-$ is of interest, as the oxidant is similar to $Co(phen)_3^{3+}$ in having a hydrophobic, π-conjugated ligand edge to facilitate interactions with hydrophobic protein regions but is vastly different in overall electrostatic charge.

Experimental Section

Reductant and oxidant solution preparations and kinetic measurements were conducted as described previously.[8] Japanese *Rhus vernicifera* stellacyanin, *Phaseolus vulgaris* plastocyanin, and *Pseudomonas aeruginosa* azurin were purified by standard methods.[2a]

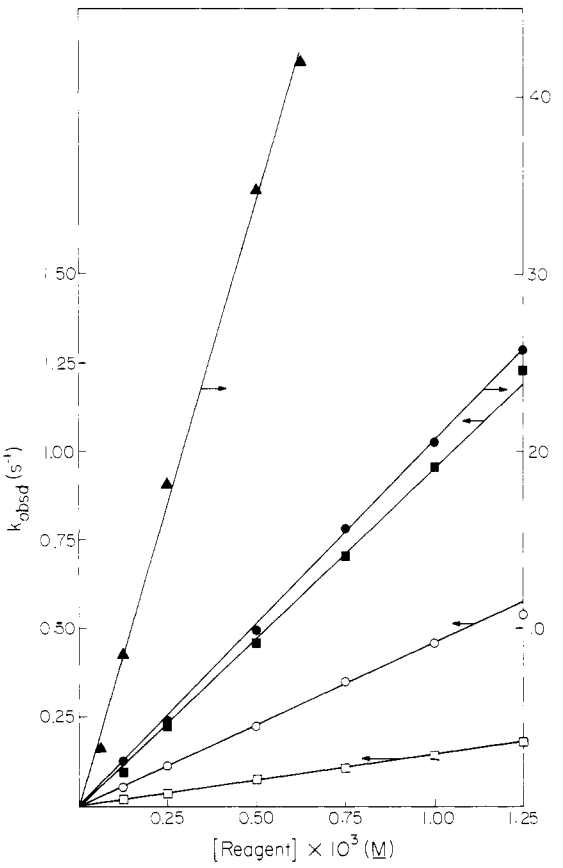

Figure 1. Dependences of the observed rate constants on reagent concentration at 25 °C [pH 7.0 (phosphate) μ = 0.2 M]: (■) $Fe(dipic)_2^{2-}$–azurin(II); (□) $Co(dipic)_2^-$–azurin(I); (●) $Fe(dipic)_2^{2-}$–plastocyanin(II); (○) $Co(dipic)_2^-$–plastocyanin(I): (▲) $Fe(dipic)_2^{2-}$–stellacyanin(II).

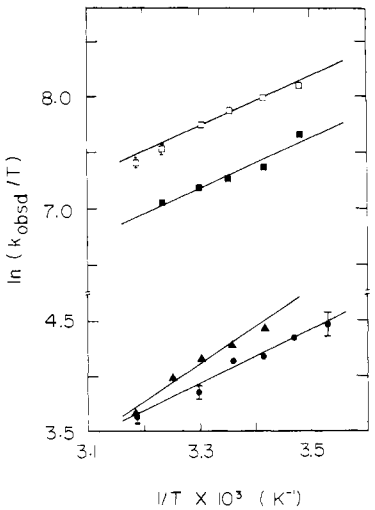

Figure 2. Eyring plots of the rate data for the reactions of $Fe(dipic)_2^{2-}$ and $Co(dipic)_2^-$ with blue copper proteins [pH 7.0 (phosphate), μ = 0.2 M]. In each case, [reagent] = 2.5 × 10^{-4} M except for stellacyanin(II)–$Fe(dipic)_2^{2-}$, where $[Fe(dipic)_2^{2-}]$ = 2.25 × 10^{-5} M. Symbols are the same as in Figure 1. Error bars are indicated in those cases where they extend beyond the dimensions of the symbol.

Preparative reduction of plastocyanin and azurin for use in oxidation studies was performed by dropwise addition of a concentrated $Fe(EDTA)^{2-}$ solution (~20 mM, pH 7) to the protein (~1 mL) until the blue color was bleached. Excess reductant and the oxidation product were than removed by quickly placing the reduced protein into a small dialysis bag and dialyzing against one change of 2000-fold excess of the appropriate argon-purged buffer at 4 °C. The protein was then diluted quickly with argon-purged buffer and bubbled slowly with argon for 20 min before being transferred into the drive syringes. Stellacyanin was

(1) (a) Department of Biochemistry, University of British Columbia, Vancouver, B.C., V6T 1W5, Canada. (b) Istituto di Chimica Generale ed Inorganica dell'Universitâ, 30123 Venezia, Italy.

(2) (a) Wherland, S.; Holwerda, R. A.; Rosenberg, R. C.; Gray, H. B. *J. Am. Chem. Soc.* **1975**, *97*, 5260. (b) Rosenberg, R. C.; Wherland, S.; Holwerda, R. A.; Gray, H. B. *Ibid.* **1976**, *98*, 6364. (c) McArdle, J. V.; Coyle, C. L.; Gray, H. B.; Yoneda, G. S.; Holwerda, R. A. *Ibid.* **1977**, *99*, 2483. (d) Holwerda, R. A.; Wherland, S.; Gray, H. B. *Ann. Rev. Biophys. Bioeng.* **1976**, *5*, 363. (e) Cummins, D.; Gray, H. B. *J. Am. Chem. Soc.* **1977**, *99*, 5188. (f) Wherland, S.; Gray, H. B. In "Biological Aspects of Inorganic Chemistry"; Addison, A. W., Cullen, W., Dolphin, D., James, B. R., Eds.; Wiley: New York, 1977; p 289. (g) Gray, H. B.; Coyle, C. L.; Dooley, D. M. et al. *Adv. Chem. Ser.* **1977**, *No.* **162**, 145.

(3) (a) Solomon, E. I.; Hare, J. W.; Dooley, D. M.; Dawson, J. H.; Stephens, P. J.; Gray, H. B. *J. Am. Chem. Soc.* **1980**, *102*, 168. (b) Gray, H. B.; Solomon, E. I. In "Copper Proteins"; Spiro, T. G., Ed.; Wiley: New York, 1981; Chapter 1.

(4) Mauk, A. G.; Scott, R. A.; Gray, H. B. *J. Am. Chem. Soc.* **1980**, *102*, 4360.

(5) (a) Segal, M. G.; Sykes, A. G. *J. Chem. Soc., Chem. Commun.* **1977**, 764. (b) Segal, M. G.; Sykes, A. G. *J. Am. Chem. Soc.* **1978**, *100*, 4585. (c) Lappin, A. G.; Segal, M. G.; Weatherburn, D. C.; Henderson, R. A.; Sykes, A. G. *Ibid.* **1979**, *101*, 2302. (d) Lappin, A. G.; Segal, M. G.; Weatherburn, D. C.; Sykes, A. G. *Ibid.* **1979**, *101*, 2297. (e) Lappin, A. G.; Segal, M. G.; Weatherburn, D. C.; Sykes, A. G. *J. Chem. Soc., Chem. Commun.* **1979**, 38.

(6) (a) Cookson, D. J.; Hayes, M. T.; Wright, P. E. *Nature, (London)* **1980**, *283*, 683. (b) Cookson, D. J.; Hayes, M. T.; Wright, P. E. *Biochim, Biophys. Acta* **1980**, *591*, 162. (c) Freeman, H. C. In "Coordination Chemistry-21"; Laurent, J. P., Ed., Pergamon: Oxford, 1981; p 29.

(7) Yoneda, G. S.; Holwerda, R. A. *Bioinorg. Chem.* **1978**, *8*, 139.

(8) Mauk, A. G.; Coyle, C. L.; Bordignon, E.; Gray, H. B. *J. Am. Chem. Soc.* **1979**, *101*, 5054.

Table I. Calculated Protein Self-Exchange Rate Constants (25 °C, μ = 0.1 M (phosphate), pH 7.0)[a]

protein	reagent	Z_1/Z_1' [b]	k_{12},[c] M^{-1} s^{-1}	w_{12} [d,e]	w_{11} [d,f]	w_{21} [d,e]	$\Delta G^{\ddagger}_{11}{}^{corr}$	$k_{11}{}^{corr}$, M^{-1} s^{-1}
plastocyanin	$Fe(dipic)_2^{2-}$	9-/10-	2.04×10^4	0.355	0.882	0.197	15.39[g]	3.2×10^1
plastocyanin	$Co(dipic)_2^-$	10-/9-	4.57×10^2	0.197	0.882	0.355	11.49[h]	2.3×10^4
azurin	$Fe(dipic)_2^{2-}$	1-/2-	9.82×10^2	0.0334	0.015	0.0334	18.23[g]	2.6×10^{-1}
azurin	$Co(dipic)_2^-$	2-/1-	1.4×10^2	0.0334	0.015	0.0334	12.89[h]	2.2×10^3

[a] The radius of a bis(dipicolinate) complex was estimated from a molecular model to be 5.2 Å; protein radii are from ref 2f (plastocyanin, 15.2 Å; azurin, 17.2 Å); w_{22} = 0.308 kcal/mol. Reduction potentials: plastocyanin, 347 mV; azurin, 330 mV; stellacyanin, 184 mV (Sailasuta, N.; Anson, F. C.; Gray, H. B. *J. Am. Chem. Soc.* 1979, *101*, 455). [b] The two charges are for the reactant and product (estimated from sequence data, ref 2f). [c] 25 °C, pH 7.0 (phosphate), μ = 0.2 M. [d] All energies in kcal/mol. [e] Work terms were calculated for the conditions of the cross reactions. [f] Work terms were calculated for 0.1 M ionic strength. [g] Calculations based on E° ($Fe(dipic)_2^{2-}$) = 278 mV and $k_{22}{}^{corr}$ = 3.2 (10^5) M^{-1} s^{-1}; the $k_{22}{}^{corr}$ was calculated from the rate constant for the stellacyanin(II)-$Fe(dipic)_2^{2-}$ reaction (see ref 2f). [h] Calculation based on E° ($Co(dipic)_2^{-/2-}$) = 400 mV and $k_{22}{}^{corr}$ = 4.0 (10^{-1}) M^{-1} s^{-1} (ref 8).

reduced with ascorbate as described previously.[2c]

Results

All first-order plots were linear for at least 90% of the reaction. The dependences of observed first-order rate constants on reagent concentration for five reactions are shown in Figure 1. At a 10-fold excess of oxidant, only the last part of the stellacyanin(I)-$Co(dipic)_2^-$ reaction could be seen. Second-order rate constants obtained from weighted linear least-squares fits of the data in Figure 1 are as follows (25 °C, pH 7.0 (phosphate), μ = 0.2 M): 6.8 (2) × 10^4, stellacyanin(II)-$Fe(dipic)_2^{2-}$; 2.04 (8) × 10^4, plastocyanin(II)-$Fe(dipic)_2^{2-}$; 4.57 (7) × 10^2, plastocyanin(I)-$Co(dipic)_2^-$; 9.8 (2) × 10^2, azurin(II)-$Fe(dipic)_2^{2-}$; 1.41 (5) × 10^2, azurin(I)-$Co(dipic)_2^-$. Eyring plots for these reactions are shown in Figure 2. Weighted linear least-squares analyses of these data yield the following activation enthalpies (kcal/mol) and entropies (eu): 6.7 (4) and −14(2) for stellacyanin(II)-$Fe(dipic)_2^{2-}$; 4.8 (4) and −23 (1) for plastocyanin(II)-$Fe(dipic)_2^{2-}$; 4.5(2) and −31.2 (8) for plastocyanin(I)-$Co(dipic)_2^-$; and 4.5 (4) and −30 (1) for azurin(II)-$Fe(dipic)_2^{2-}$.

Measurements of k_{obsd} values were extended to higher reagent concentrations for the reactions of plastocyanin(I) and azurin(I) with $Co(dipic)_2^-$. In the case of plastocyanin(I), the dependence of k_{obsd} on oxidant concentration was found to be linear up to 5 mM at 25 °C. A similar investigation of the oxidation of azurin(I) at four different temperatures, however, revealed slight deviations from linearity in the k_{obsd} vs. $[Co(dipic)_2^-]$ plot (Figure 3).

As noted earlier, one mechanism consistent with rate saturation involves formation of a redox-active precursor complex:

$$\text{azurin(I)} + Co(dipic)_2^- \overset{K}{\rightleftharpoons} [\text{azurin(I)}\text{-}Co(dipic)_2^-]$$

$$[\text{azurin(I)}\text{-}Co(dipic)_2^-] \xrightarrow{k_{et}} [\text{azurin(II)}\text{-}Co(dipic)_2^{2-}]$$

$$[\text{azurin(II)}\text{-}Co(dipic)_2^{2-}] \xrightarrow{\text{fast}} \text{azurin(II)} + Co(dipic)^{2-}$$

A plot of k_{obsd}^{-1} vs. $[Co(dipic)_2^-]^{-1}$ yields k_{et} (1/intercept) and K (k_{et}/slope). Analysis of the 25 °C data (Figure 3) by a weighted linear least-squares fit to such a plot produces the following values: k_{et} = 3.3 (4) s^{-1}; K = 46 (5) M^{-1}. Extension of the analysis to include the temperature dependences gives $\Delta H^{\ddagger}$ = 11 (1) kcal/mol, $\Delta S^{\ddagger}$ = −18 (5) eu, ΔH° = −7 (1) kcal/mol, and ΔS° = −16 (5) eu.

A bimolecular electron-transfer pathway that is turned off by the formation of a redox-inactive or dead-end (de) complex is kinetically indistinguishable from the redox-active precursor mechanism:[9]

$$\text{azurin(I)} + Co(dipic)_2^- \overset{K_{de}}{\rightleftharpoons} [\text{azurin(I)}\text{-}Co(dipic)_2^-]_{de}$$

$$\text{azurin(I)} + Co(dipic)_2^- \xrightarrow{k_{12}'} \text{azurin(II)} + Co(dipic)_2^{2-}$$

(9) A third candidate mechanism involving activation of a redox-inactive form of azurin(I) to a reactive species, azurin(I)*, also could account for the apparent rate saturation, but it is inconsistent with the finding that the first-order limiting rate constant depends on the nature of the oxidant (3.3 (4) s^{-1} for $Co(dipic)_2^-$; 1.9 × 10^1 s^{-1} for $Co(phen)_3^{3+}$). Thus it is unlikely that an azurin(I)* pathway contributes significantly to the overall electron-transfer rate.

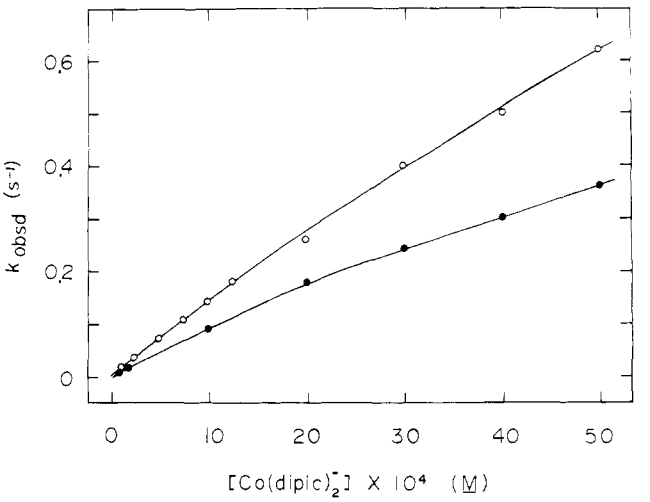

Figure 3. Dependence of k_{obsd} on $[Co(dipic)_2^-]$ for the oxidation of azurin(I) at high reagent concentrations [pH 7.0 (phosphate), μ = 0.2 M]: (○), 25 °C; (●), 10 °C. Error bars fall within the dimensions of the symbols. Data at 14 and 20 °C are given in the supplementary material section.

A double-reciprocal plot yields k_{12}' (1/slope) = 1.51 (2) × 10^2 M^{-1} s^{-1} and K_{de} (intercept/slope) = 46 (5) M^{-1} at 25 °C. The thermodynamic parameters extracted from the temperature-dependent data are the following: $\Delta H^{\ddagger}$ = 4.4 (2) kcal/mol, $\Delta S^{\ddagger}$ = −33.7 (7) eu, ΔH° = −7 (1) kcal/mol, and ΔS° = −16 (5) eu.

Electrostatics-corrected self-exchange rate constants ($k_{11}{}^{corr}$) for the blue copper proteins were calculated as described previously.[2f] For the reaction of azurin(I) with $Co(dipic)_2^-$, the k_{12}' from the bimolecular dead-end complex analysis was used for these calculations. The results including work terms are listed in Table I. To facilitate the discussion of these results, we have calculated a protein electron-transfer distance (R_p)[4] for each reagent–protein pair in the framework of the bimolecular mechanistic model (Table II). We also have included in Table II the results of similar analyses of the kinetics of reactions involving plastocyanin and azurin with other inorganic redox agents.

Discussion

Our analysis of the electron-transfer kinetics of plastocyanin and azurin shows that the inorganic redox agents fall into two broad reactivity categories. The complexes that facilitate electron transfer from the copper center are $Co(phen)_3^{3+}$ and $Co(dipic)_2^-$; these Co(III) oxidants yield k_{11}^∞ values that are several orders of magnitude larger than those based on oxidation of the proteins by $Co(ox)_3^{3-}$. Included with $Co(ox)_3^{3-}$ in the poor electron-transfer-agent group are $Fe(EDTA)^{2-}$ and $Fe(dipic)_2^{2-}$, with the latter reductant giving slightly higher k_{11}^∞ values. The overall k_{11}^∞ order is $Co(dipic)_2^- \sim Co(phen)_3^{3+} >> Fe(dipic)_2^{2-} > Fe(EDTA)^{2-} > Co(ox)_3^{3-}$ for both proteins.

Both $Co(phen)_3^{3+}$ and $Co(dipic)_2^-$ possess hydrophobic, π-conjugated ligands that could facilitate electron transfer by penetration of the protein surface to a point near the copper redox center. The viability of this mechanistic proposal is enhanced by

Table II. Calculated k_{11}^{∞} and R_p Values for Plastocyanin and Azurin Electron-Transfer Reactions

protein	reagent[a]	k_{12}^{∞}, M^{-1} s^{-1}	k_{22}^{∞}, M^{-1} s^{-1}	ΔE_{12}^{∞}, V	k_{11}^{∞}, M^{-1} s^{-1}	R_p, Å
plastocyanin	$Co(dipic)_2^-$	6.4×10^2	6.7×10^{-1}	0.05	1.0×10^5	2.2
	$Co(phen)_3^{3+}$ (de)	1.2×10^3	9.8×10^1	0.01	1.1×10^4	2.9
	$Fe(dipic)_2^{2-}$	3.7×10^4	5.4×10^5	0.08	1.4×10^2	4.5
	$Fe(EDTA)^{2-}$	1.7×10^5	6.9×10^4	0.24	7.3×10^1	4.7
	$Co(ox)_3^{3-}$	3.8×10^{-1}	1.6×10^{-5}	0.22	2.1×10^0	5.9
azurin	$Co(dipic)_2^-$ (de)	1.5×10^2	6.7×10^{-1}	0.07	2.2×10^3	3.5
	$Co(phen)_3^{3+}$ (de)	2.8×10^3	9.8×10^1	0.04	1.9×10^4	2.8
	$Fe(dipic)_2^{2-}$	1.0×10^3	5.4×10^5	0.05	2.7×10^{-1}	6.6
	$Fe(EDTA)^{2-}$	1.4×10^3	6.9×10^4	0.21	1.1×10^{-2}	7.8
	$Co(ox)_3^{3-}$	3.1×10^{-2}	1.6×10^{-5}	0.24	6.8×10^{-3}	7.9

[a] Second-order rate constants and reduction potentials for reactions involving bis(dipicolinate) complexes are given in Table I; (de), analysis assuming a dead-end complex; $Co(phen)_3^{3+}$ data: ref 5b and 5c; $Co(ox)_3^{3-}$ data: Holwerda, R. A.; Knaff, D. B.; Gray, H. B.; Clemmer, J. E.; Crowley, R. J.; Smith, J. M.; Mauk, A. G. *J. Am. Chem. Soc.* 1980, *102*, 1142.

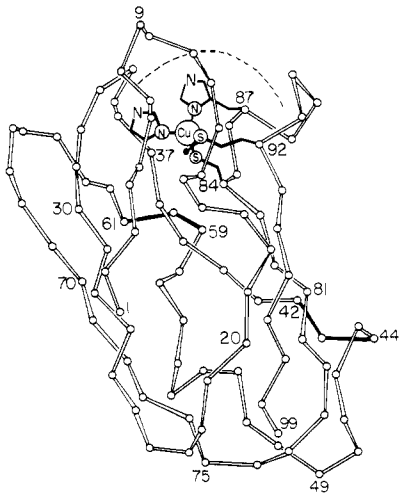

Figure 4. Representation of the α-carbon skeleton and copper ligand redox unit of plastocyanin is based on the crystal-structure analysis of the poplar protein (ref 6c). The dashed curve around the copper ligand His-87 is the assumed reagent close-contact region in the bimolecular electron-transfer mechanistic model. The azurin structure may be represented in a similar way, with the copper (His-117) unit in the reagent contact region (below the dashed curve) shielded by three residues (Met-13, Met-44, Phe-114). The "negative patch" of plastocyanin referred to in the text is formed by two groups of carboxylate residues (positions 42–45 and 59–61 in the skeleton). The analogous region in azurin contains hydrophobic residues (ref 10).

our findings for plastocyanin(I)–$Co(dipic)_2^-$. Because there is no evidence for $Co(dipic)_2^-$–protein binding, a bimolecular close-contact mechanism is the only reasonable possibility; the hydrophobic region around the copper ligand His-87 is the obvious choice for the reagent contact site (Figure 4). It is important to point out that *binding does not give Co(phen)$_3^{3+}$ any reactivity advantage over Co(dipic)$_2^-$*. For this reason, it would be unwise to dismiss the bimolecular dead-end interpretation of the $Co(phen)_3^{3+}$ saturation kinetics. At this point we favor a mechanistic model in which $Co(phen)_3^{3+}$ utilizes the same plastocyanin electron-transfer site as does $Co(dipic)_2^-$, namely, the hydrophobic region very near His-87 (and the copper atom).

The kinetics of the reactions of azurin(I) with $Co(phen)_3^{3+}$ and $Co(dipic)_2^-$ also may be interpreted in a straightforward manner in terms of the bimolecular close-contact pathway (Table II). At the very least, a significant contribution to the overall electron-transfer rate must come from the close-contact pathway, which presumably involves reagent penetration in the hydrophobic region near the copper ligand His-117.[10] The nature of the azurin binding site associated with rate saturation in each case is not known, but on the basis of the absence of a cluster of charged residues on the surface (i.e., there is no "negative patch" nor is there a grouping of positively charged residues),[10] it is reasonable to assume that it is a hydrophobic region. One intriguing possibility is that the oxidants bind to azurin(I) in the extensive hydrophobic region that effectively replaces the plastocyanin negative patch.[6c,10]

For both plastocyanin and azurin there is a surprisingly large difference in the apparent reactivities of $Co(dipic)_2^-$ and $Fe(dipic)_2^{2-}$. One reasonable possibility is that the low-spin Co(III) redox center is distorted during formation of a reagent–protein (penetration) complex, thereby lowering the large inner-sphere reorganization barrier to electron transfer.[8] In our analysis such a decrease in the activation barrier would appear as an anomalously large k_{11}^{∞} and a correspondingly small R_p. That the extent of penetration of $Co(dipic)_2^-$ may be overestimated in our model receives some support from an examination of the activation parameters for the reactions of plastocyanin and azurin with $Fe(dipic)_2^{2-}$ and $Co(dipic)_2^-$. The $\Delta H^{\ddagger}$ and $\Delta S^{\ddagger}$ values for each protein are very similar for both reduction and oxidation reactions, implying that similar mechanisms are involved. Indeed, the relatively small $\Delta H^{\ddagger}$'s and the large negative $\Delta S^{\ddagger}$'s for the protein oxidations by $Co(dipic)_2^-$ are readily reconciled by a mechanistic model in which partial activation of the Co(III) center accompanies a relatively small degree of reagent penetration.[11]

The interpretation of the estimated electron-transfer distances for the reactions of plastocyanin and azurin with the poor reagents is relatively straightforward. There is no evidence for reagent–protein binding in these cases, so a bimolecular pathway is the only reasonable choice. The R_p values for $Fe(EDTA)^{2-}$ reductions and $Co(ox)_3^{3-}$ oxidations are 2–3 Å larger for azurin than for plastocyanin, thereby indicating that these hydrophilic reagents cannot penetrate the hydrophobic regions around the histidine-copper electron-transfer units. Longer electron-transfer distances are involved for azurin, because three residues (Met-13, Met-44, Phe-114)[10] shield the Cu(His-117) unit from direct contact with solvent (or other external) molecules. The plastocyanin molecule[6c] does not provide similar protective partners for His-87.

Acknowledgment. A.G.M. acknowledges National Institutes of Health Postdoctoral Fellowship AM05760-02 (1977–79) and a grant from Medical Research Council of Canada (MA-7182). E. B. acknowledges a travel grant from NATO. This research was supported by National Science Foundation Grant CHE80-24863.

Registry No. $Co(dipic)_2^-$, 71605-21-5; $Fe(dipic)_2^{2-}$, 71605-20-4.

Supplementary Material Available: Listing of observed pseudo-first-order rate constants (2 pages). Ordering information is given on any current masthead page.

(10) Adman, E. T.; Jensen, L. H. *Isr. J. Chem.* **1981**, *21*, 8.

(11) Note, however, that it is likely that a significant contribution to each negative $\Delta S^{\ddagger}$ comes from the interaction of the two negatively charged reactants, thereby ordering solvent molecules in the activated complex. This $\Delta S^{\ddagger}$ (solvation) may mask other effects that contribute to $\Delta S^{\ddagger}$ in the plastocyanin and azurin reactions.